Available online at www.sciencedirect.com

ScienceDirect

Journal of Magnesium and Alloys 1 (2013) 249–255
www.elsevier.com/journals/journal-of-magnesium-and-alloys/2213-9567

Full length article

Effect of rare earth and Mn elements on the corrosion behavior of extruded AZ61 system in 3.5 wt% NaCl solution and salt spray test

Shijie Zhu*, Zhidan Liu, RuiXiao Qu, LiGuo Wang, Qingkui Li, Shaokang Guan**

School of Materials Science and Engineering, Zhengzhou University, 100 Science Road, Zhengzhou 450001, China

Received 21 August 2013; revised 17 October 2013; accepted 17 October 2013

Abstract

In this study, multiple addition of rare earth (RE) and manganese (Mn) to AZ61 was conducted aiming to find out the influence to corrosion resistance. AZ61 containing different amounts of RE and Mn was investigated by electrochemical measurement in condition of 3.5 wt% NaCl solution at 25 °C. Gravimetric measurement was conducted in 5 wt% salt spray at 35 °C and 3.5 wt% NaCl solution at 25 °C. Samples were characterized by SEM, EDS, OM and XRD. The result shows that with RE addition Al_8Mn_5 in AZ61 changed into $Al_{10}RE_2Mn_7$. The quantity of β phase is reduced significantly. The multiple addition of RE and Mn improved the corrosion resistance of AZ61. When the ratio of Mn and RE is 0.3, alloy has the best property of corrosion resistance. In addition, the composite addition removed the impurity elements in AZ61 especially Fe.

Keywords: AZ61; Rare earth; Multiple addition; Corrosion resistance; Electrochemical properties

1. Introduction

Magnesium alloy has the advantages of lightweight, high specific strength and specific stiffness. In the background of lacking energy and urgent need for lightweight and energy-efficient, it's an ideal measure that the use of magnesium alloy on vehicles is broadened to deal with this problem [1,2]. However, low corrosion resistance and strength relatively confine the application of magnesium alloy. It is important that magnesium alloy should have adequate corrosion resistance before using in aircraft and mobile industry. However, there is a great difference in electrode potential between α-Mg matrix and other metals, intermetallic compounds and phases. Forming of many small quite effective local cells leads α-Mg dissolution as positive electrode. Especially, dissolution of α-Mg is accelerated when chloride is existing, so observation of alloy in immersion test of NaCl solution or salt spray test is necessary [3]. Currently, researchers generally optimize the alloy composition [4], use advanced processing technology and obtain better surface protection to improve the corrosion resistance of magnesium alloy [5].

Mg–Al–Zn magnesium alloy has the characters of low processing cost and a wide range of application [6]. But corrosion resistance of ordinary Mg–Al–Zn magnesium alloy isn't passable, especially only serving a short time in some of the high-salt, high temperature or humid environment will cause component failure due to corrosion, thus it will limit its scope of application.

* Corresponding author. Tel.: +86 371 63887508; fax: +86 371 67781593.
** Corresponding author. Tel.: +86 371 67780051; fax: +86 371 67780050.
E-mail addresses: zhusj@zzu.edu.cn (S. Zhu), skguan@zzu.edu.cn (S. Guan).

Peer review under responsibility of National Engineering Research Center for Magnesium Alloys of China, Chongqing University.

Production and hosting by Elsevier

http://dx.doi.org/10.1016/j.jma.2013.10.003.

Table 1
Test results by direct reading spectrometer before casting.

Num	Al	Zn	Mn	RE	Fe	Mn/RE	Mg
CMPT 1	5.84	0.81	0.30	–	0.0042	–	Bal.
CMPT 2	5.60	0.94	0.73	0.39	0.0012	1.87	Bal.
CMPT 3	5.69	0.85	0.68	0.67	0.0014	1.01	Bal.
CMPT 4	5.66	0.93	0.62	0.80	0.0010	0.78	Bal.
CMPT 5	5.64	0.93	0.54	0.91	0.0013	0.59	Bal.
CMPT 6	5.74	0.98	0.30	1.00	0.0014	0.30	Bal.

An important factor that affects corrosion resistance of magnesium alloy is the presence of impurity elements, for instance Fe, Ni, Cu, etc. To reduce the content of these impurities can significantly improve the corrosion resistance of magnesium alloy. Study found that if magnesium alloy melt can be purified effectively and the surface protection process was carried out well, devices made of magnesium alloy can replace the ones made of conventional aluminum alloy substantially [7,8].

In this study, multivariate alloying was invested in Mg–Al–Zn magnesium alloy. In the following, several major alloying elements which are often used in Mg–Al–Zn magnesium alloy are listed.

1.1. Manganese (Mn) [9]

Its maximum solid solubility in magnesium is of 2.2%. Normally, Mn is added in the form of Mg–Mn intermediate alloy or $MnCl_2$ to magnesium. Complex Mg–Fe–Mn compound precipitates will form to remove impurity iron existing in magnesium alloy melt. It can also be seen as alloying elements to improve resistance to corrosion. In addition, with the forming of spherical phase containing manganese and aluminum, mechanical properties of magnesium alloy can also be improved to a certain extent.

1.2. Cerium (Ce) [10]

When Ce is added into Mg–Al–Zn magnesium alloy, continuous mesh β phases become granular or discontinuous mesh-like distributing in the grain boundaries. Then the distribution is more diffuse, the number of β phase significantly decreased. It can greatly increase the corrosion resistance of Mg–Al–Zn magnesium alloy when there is a significant reduction of β phase and a purification of the substrate as well as the cerium oxide-rich film formed.

1.3. Lathanum (La) [10]

When the La element is added into Mg–Al–Zn magnesium alloy, undercooling of solid–liquid interface will increase greatly, thereby the cast grain will be refined. Appropriate amount of La element can also make the β phase grainy distribution or discontinuous distribution. Addition of La element is the same to Ce to purify the melt and form stable protective film to increase the corrosion resistance of magnesium alloy substantially.

Moreover, cerium-rich mixed rare earth is low-cost and suitable for industrial production. Based on AZ61, wrought magnesium alloy with better corrosion resistance should be developed.

2. Experimental

2.1. Test materials

Raw materials including magnesium (99.95%), aluminum, zinc and $MnCl_2$ were gotten from WINCA Magnesium Co., Ltd. The rare earth (99.9%, Baotou Steel Rare Earth (Group) Hi-tech Co., Ltd., China) contains cerium (Ce) 65%, neodymium (Nd) 10%, lanthanum (La), 20%, and small amount

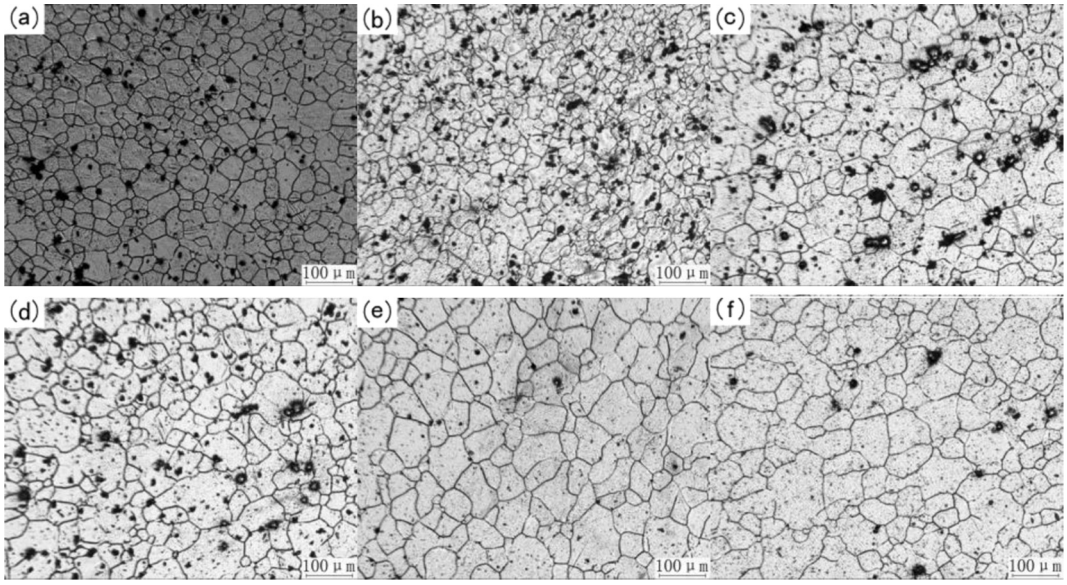

Fig. 1. The metallographic microstructure of cross-section.

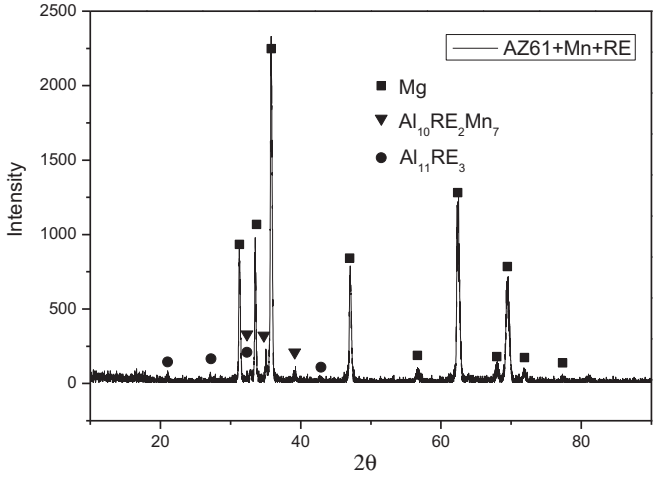

Fig. 2. XRD pattern of extruded AZ61 + Mn + RE.

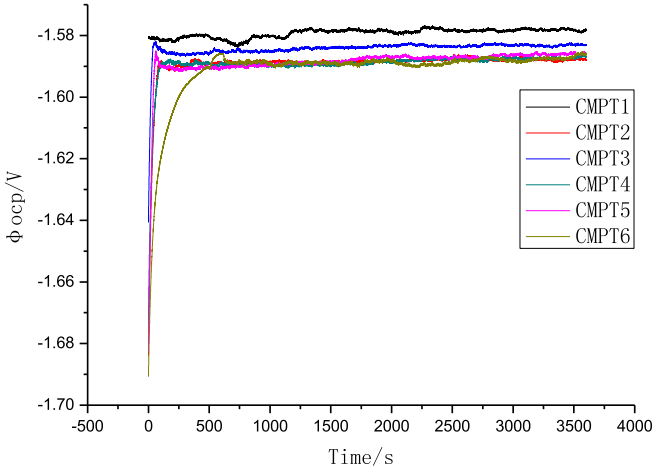

Fig. 3. Open circuit potential of AZ61 and of AZ61 + Mn + RE.

of praseodymium (Pr), 5%. When melting, metals and $MnCl_2$ are under the protection of CO_2 and SF_6 with ratio of 95:5. Solvent II was put into electrical furnace with a capacity of 100 kg. Billets (φ120 mm × 1000 mm) were cast by flat die. After inspection through BLC-2000 ultrasonic non-destructive flaw, billets were homogenized at 420 °C ± 5 °C for 12 h in box-type resistance furnace and then processed into φ112 × 420 mm by lathe. Porthole die was used to extrude billets into bars with size of φ20 ± 0.05 mm at 430 °C. The extrusion ratio is 31.4 and bar extrusion rate is 2.5 m/min.

The following in Table 1 is an alloy composition list got by Swiss ARL3460 direct reading spectrometer, wherein component 1 is AZ61 magnesium alloy without rare earth. Components from 2 to 6 were added into Mn and RE elements with different proportions. The Mn/RE ratios are 1.87, 1.0, 0.775, 0.593 and 0.305 respectively.

2.2. Specimen preparation and characterization

Metallographic equipments were used including PG-1a metallographic sample polishing machine and Olympus H2-UMA metallurgical microscope. The electrochemical experimental equipment is RST5000 electrochemical workstation. SEM and EDS analysis was carried out by Philips Quanta-2000. Philips 1700X was used for X-ray diffraction (XRD) study.

In the corrosion experiment, the corrosion rate was measured by DCTC-600P salt spray corrosion test chamber according to ASTM B117-73.

3. Results and discussion

In conjunction with Mg–Fe binary phase diagram, it shows that the presence of iron in magnesium is in the form of α-Fe. The solubility of α-Fe in magnesium is extremely small at room temperature. However, the addition of Mn can remove iron element in magnesium alloy effectively, furthermore rare earth elements, especially light rare earth elements also have the function of scavenging impurities containing iron element to some extent. In Table 1, it shows that through multiple addition of Mn and RE elements, iron element in AZ61 magnesium alloy was reduced from 0.0042 wt% after manganese was added alone to below 0.0015 wt% after the multiple addition of Mn and RE elements, wherein Fe element as low as 0.001 wt%. By this way, magnesium alloy was further purified and the composite addition reduced the Fe content in the magnesium alloy significantly.

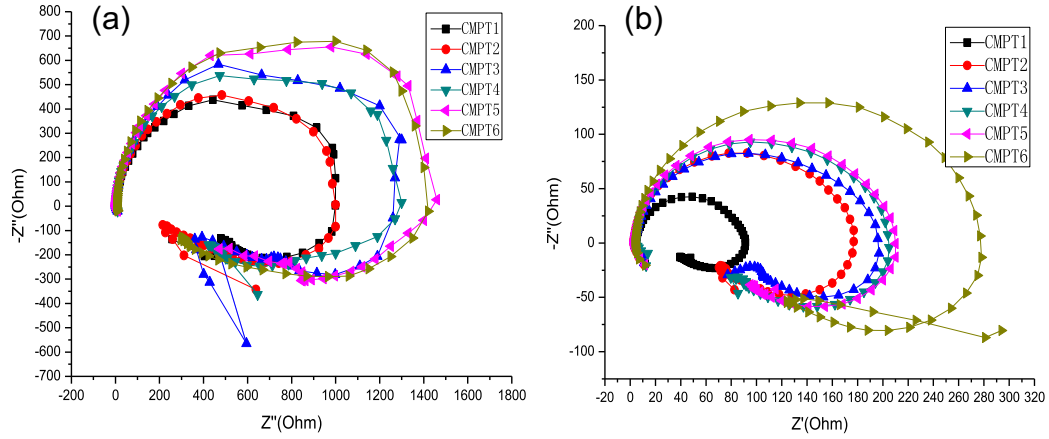

Fig. 4. (a) EIS of AZ61 and AZ61 + Mn + RE. (b) EIS after immersion in 3.5% NaCl solution for 1 h.

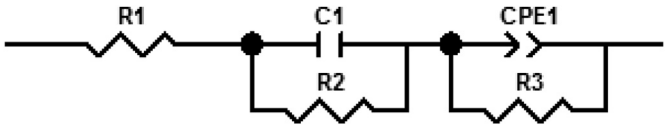

Fig. 5. The equivalent circuit diagram.

Table 2
Fitting results of EIS.

Number	R1	C1(E−5)	R2	CPE1-T(E-7)	CPE1-P	R3
CMPT1	3.0530	−2.6279	84.44	6.3033	1.282	1.6690
CMPT2	0.45612	−2.1445	168.8	3.9524	1.267	2.4330
CMPT3	2.7990	−2.0197	176.1	2.4073	1.400	1.2590
CMPT4	3.5750	−2.1616	192.2	4.2594	1.454	0.78426
CMPT5	2.0560	−2.1470	196.9	3.6488	1.347	1.5760
CMPT6	2.3640	−2.1237	265.2	2.8491	1.397	1.3290

3.1. The microstructure and second phase

In Fig. 1, those are microstructures of cross-section of extruded AZ61 and AZ61 + Mn + RE magnesium alloy. In panels (a) and (b), there are smaller uniform grains than others. With the variation of Mn/RE ratio, the grain size of extruded AZ61 magnesium alloy becomes larger gradually, and the deviation of the grain size also increases. Combined with Fig. 2, the second phase like black dot in Fig. 1 is Al_8Mn_5 or $Al_{10}RE_2Mn_7$. After observation, it is found that these phases mainly present at the grain boundaries and only a small amount of them distribute in the interior. It is inferred that the dynamic recrystallization nucleation occurs at grain boundaries following by formation and migration of a new high angle grain boundary, and ultimately stop at the point of Al_8Mn_5 or $Al_{10}RE_2Mn_7$.

3.2. Electrochemical measurements

3.2.1. Open circuit potential

As shown in Fig. 3, when RE and Mn elements are added into magnesium alloy, their open circuit potential values are generally more negative than AZ61. The main reason may be that AZ61 + Mn + RE magnesium alloy has more broken second phase containing rare earth element existing at the surface and the second phase which contains rare earth shows more chemical activity than other phases in AZ61, so it will act as anode in micro-galvanic reaction first. Then the formation of a micro-cell makes its surface more active, while AZ61 contains less second phase with lower chemical activity, so their open circuit potential is higher. But this phenomenon cannot reveal that the corrosion performance of AZ61 is better than other several components, but only the corrosion tendency is lower.

3.2.2. Electrochemical impedance spectroscopy and fitting

In Figs. 4 and 5, those are impedance spectroscopies of AZ61 and AZ61 + Mn + RE under the condition of no treatment and soaked for 1 h respectively. Theoretically, impedance spectroscopies are consisted by a high-frequency capacitive loop and a low-frequency capacitive loop.

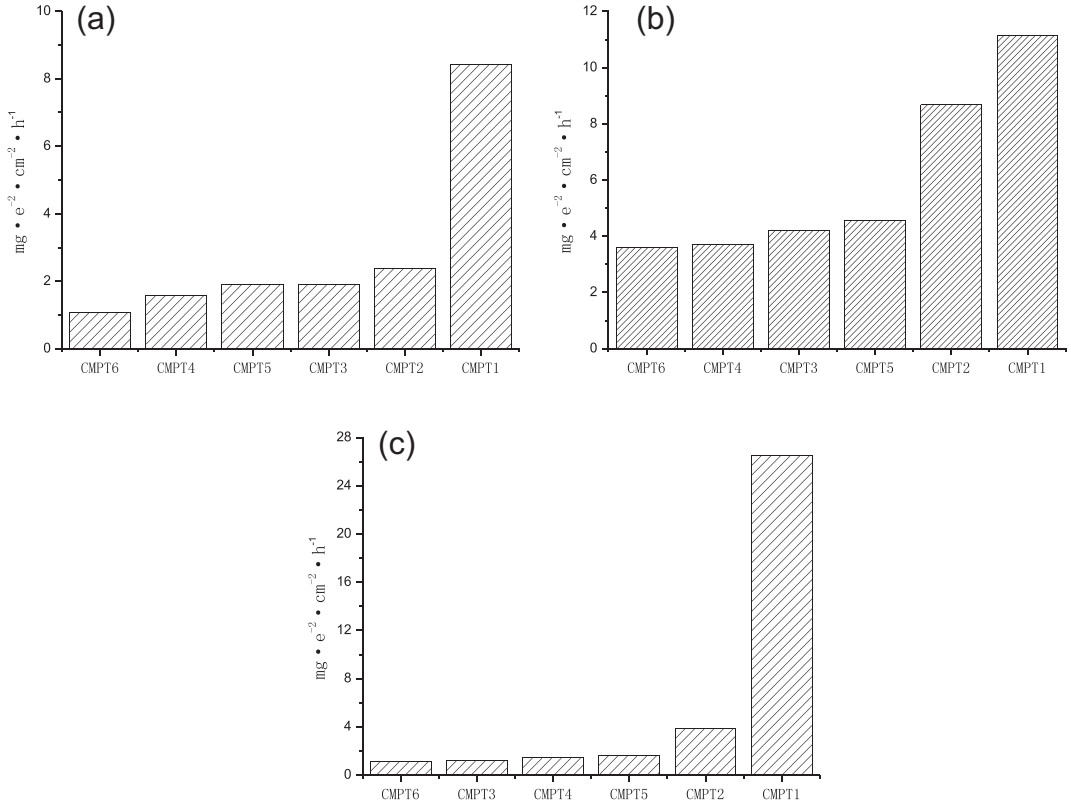

Fig. 6. Corrosion rate for different immersion times: (a) 72 h; (b) 6 d; (c) 12 d.

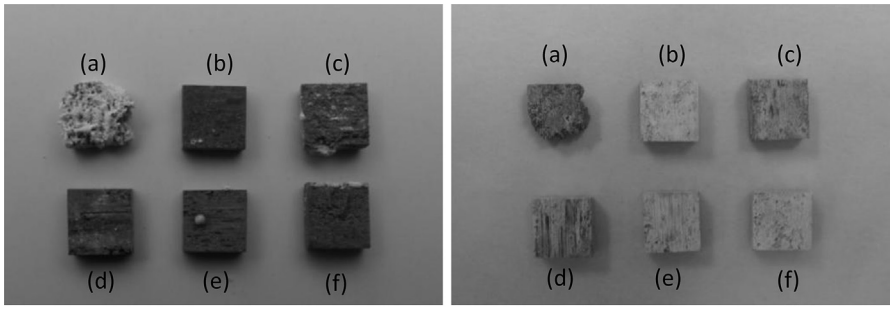

Before the removal of corrosion products Ater the removal of corrosion products

Fig. 7. Comparison before and after the removal of corrosion products after immersion for 12 d.

However, there is also a low frequency inductance loop in each EIS plot. Generally, the surface of magnesium alloy is always oxidized to form an oxide film inevitably. In this situation, when magnesium alloy reacts as anode and dissolves, the protection film is destroyed locally.

Equivalent circuit diagram of part of electrode process is obtained through fitting by software which is shown in Fig. 5. It is composed by three equivalent resistances R1, R2 and R3, an equivalent capacitance C1 and a constant phase angle element CPE1. For the double impedance of solid electrodes is not completely consistent with the equivalent capacitance impedance and the latter part exists some deviation called "dispersion effect", so in order to eliminate this effect, a constant phase element CPE is added.

For magnesium alloy, in the equivalent circuit, the impedance behavior of surface film is simulated by part consist with film resistors R2 and membrane capacitance C1. The other part consists of charge transfer resistor R3 and electric double layer capacitor CPE1 simulates corrosion electrochemical process. Theoretically, the larger the surface film resistor R2 value is, the stronger the ability of surface film protects magnesium matrix. The greater the charge transfer resistor R3 value is, the easier the resistance of electrochemical corrosion is blocked (Table 2).

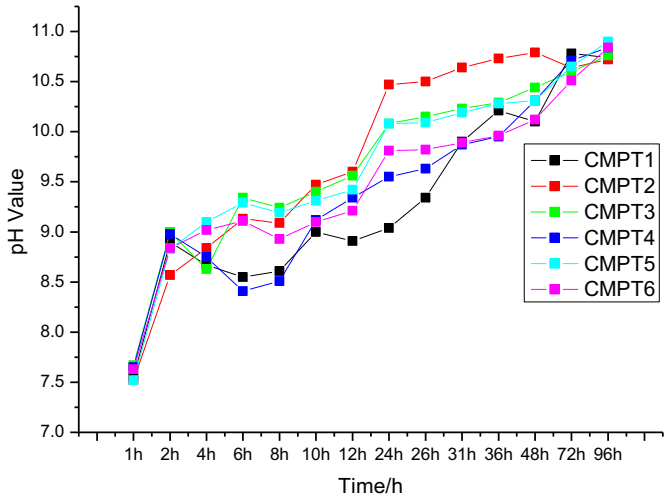

Fig. 8. Curves of pH value changing with the immersion time.

3.3. Gravimetric measurement

3.3.1. Immersion test in 3.5 wt% NaCl solution

In this experiment, to maintain the test temperature, the temperature of water bath was set to 25 °C ± 1 °C. The following is corrosion rate of each component in 3.5 wt% NaCl solution for 3, 6 and 12 days. As shown in Fig. 6, by immersion for different times, it was found that with the prolongation of immersion time corrosion rate of AZ61 was accelerated, however other components had a rapid corrosion rate in the early but the corrosion rate slowed down with protection film forming and stabilized. Except for AZ61, other components have a corrosion rate change process of first increases and then decreases, so it could be inferred that when soaked in 3.5 wt% NaCl for 12 days, those components have been formed passivation protection film [11].

Fig. 7 below shows sample morphology comparison of AZ61 and AZ61 + Mn + RE magnesium alloy before and after the removal of corrosion products. In this picture, (a)–(f) represent component 1 to component 6. The left one is macromorphology photo after immersion and the right one is picture of the surface after removing corrosion products using chromium oxide and silver nitrate.

It could be seen that the corrosion type is still pitting. After removal of corrosion products there are varying amounts of corrosion pits for different components. From the perspective of electrochemical, pitting on the surface cannot be avoided easily. In 3.5 wt% NaCl solution, the localized corrosion potential of AZ61 magnesium alloy is generally more negative than the self corrosion potential, so in AZ magnesium alloy localized corrosion damage occurs first instead of the uniform corrosion.

When corrosion products of AZ61 and AZ61 + Mn + RE magnesium alloy are not removed, white protrusions of corrosion products can be observed on the surface since the dissolution and deposition of $Mg(OH)_2$ under the action of chlorine ions. There are many corrosion pits under corrosion products. That is because protective film did not form on the pitting. Moreover, hydrogen evolution and $Mg(OH)_2$

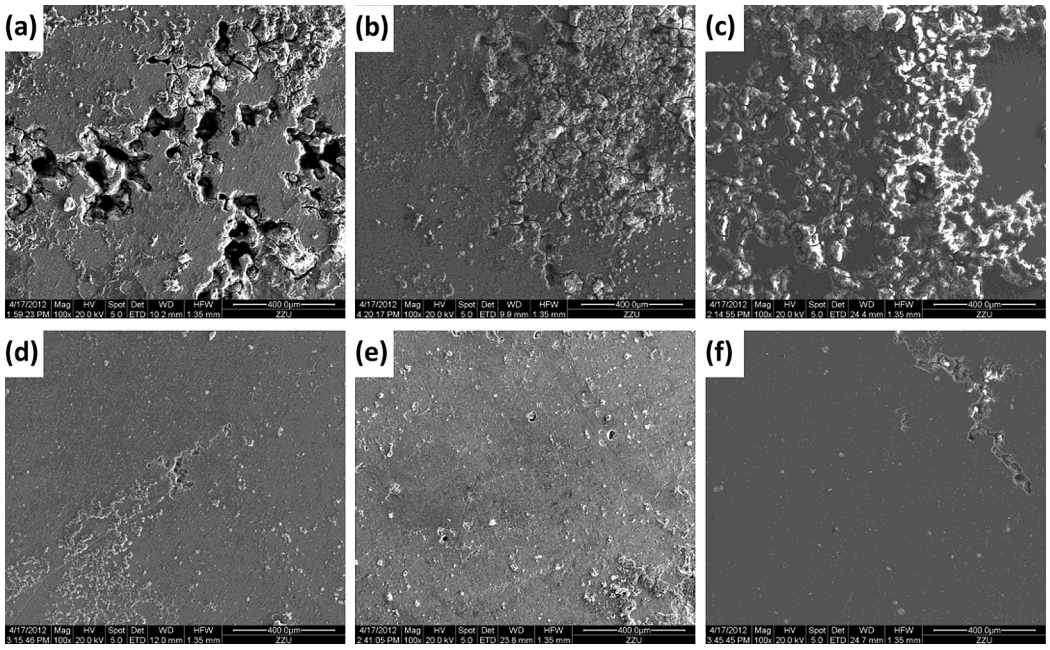

Fig. 9. The surface morphology after salt spray test.

dissolving are easier. However, deep corrosion pits didn't form on the surface of AZ61 + Mn + RE. As shown in Fig. 8, the pH value of the solution was alkaline and gradually increased around pits, so depth of corrosion pits was inhibited to some extent.

3.3.2. Salt spray test

In this experiment, 5 wt% NaCl solution is used as a corrosion media according to ASTM B117-73. The test time is of 72 h. It could be seen that oxide film of AZ61 is very easy to fall off in Fig. 9(a) after it was ashed with distilled water. With the Mn/RE ratio changing, the extent of corrosion to AZ61 + Mn + RE magnesium alloy in salt spray test was reduced gradually.

It can be determined by means of surface element scanning that second phase next to corrosion pits was $Al_{10}RE_2Mn_7$ as shown in Fig. 10. This prevented further expansion of corrosion along the planar direction.

After salt spray test, corrosion product was removed by chromic acid solution. In the salt spray test, the corrosion rate of magnesium alloys is shown in Fig. 11. Component 6 has the lowest corrosion rate, while AZ61 corrosion rate is up to approximately 6 times than that of component 6 and then followed by component 2, however there is little difference

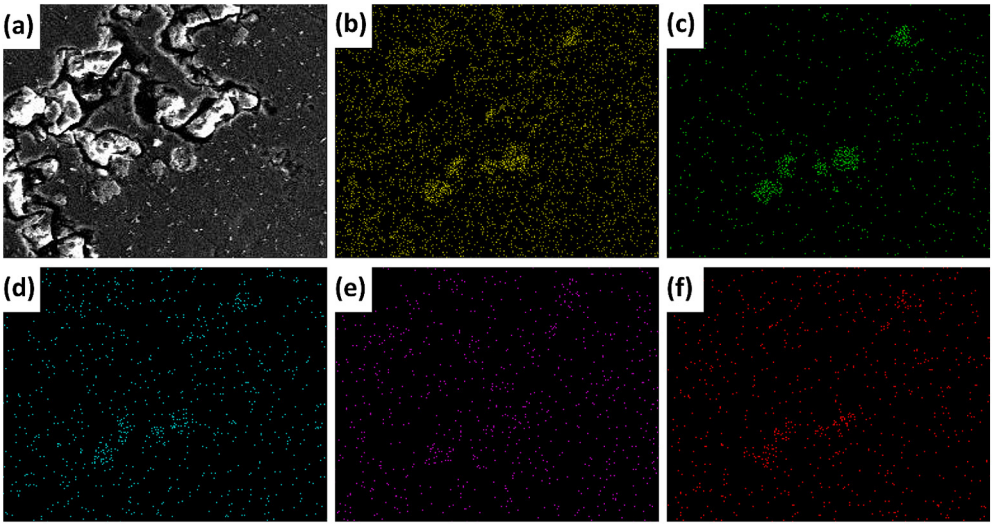

Fig. 10. Main elements scan of salt spray corrosion surface. (a) Matrix; (b) Al; (c) Mn; (d) Ce; (e) La; (f) Nd.

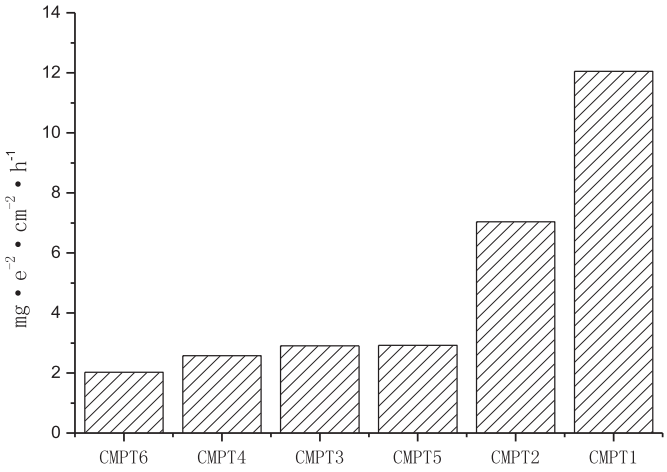

Fig. 11. The corrosion rate of salt spray test for 72 h.

between the other three components. This result is consistent with immersion test of 3.5 wt% NaCl solution.

4. Conclusion

The morphology of β phase changed and its number decreased after multiple addition of RE and Mn. Corrosion rate changed with different Mn/RE ratio and has process of increased at first and then decreased.

According to OCP curves, the surface of AZ61 + Mn + RE is more active than that of AZ61 and have good performance of corrosion resistance in initial stage of corrosion.

For the impedance, according to data obtained from the fitting, corrosion resistance from component 1 to component 6 gradually increased substantially.

Corrosion rate of AZ61 accelerated with the increasing of immersion time and corrosion rate of other magnesium alloy was rapid in the initial stage of corrosion but slowed down later. Result of salt spray test is general in line with salt water immersion test results. Compound addition of Mn and RE improved the corrosion resistance of AZ61, especially when the ratio reaches to 0.67. However, when the ratio increases, the corrosion resistance continues to improve but slightly.

Multiple addition of Mn and RE reduced iron content in magnesium greatly. Iron content reduced from 0.0042wt% when Mn element was added separately, to 0.0015wt% when both Mn and RE elements were added, wherein the lowest Fe content is 0.001 wt%.

Acknowledgments

The authors are grateful for the support by National Key Technology R&D Program of China (No. 2011BAE22B04) and the National Natural Science Foundation of China (No. 51171174).

References

[1] K.U. Kainer (Ed.), Magnesium – 8th International Conference on Magnesium Alloys and their Applications, WILEY-VCH Verlag, Weinheim, 2009.
[2] Alan A. Luo, J. Magnesium Alloys 1 (2013) 2–22.
[3] R. Arrabal, A. Pardo, M.C. Merino, M. Mohedano, P. Casajus, K. Paucar, G. Garces, Corros. Sci. 55 (2012) 301–312.
[4] C. Blawert, D. Fechner, D. Hoche, V. Heitmann, W. Dietzel, K.U. Kainer, P. Zivanovic, C. Scharf, A. Ditze, J. Grobner, R. Schmid-Fetzer, Corros. Sci. 52 (2010) 2452–2468.
[5] J.E. Gray, B. Luan, J. Alloys Compd. 336 (2002) 88–113.
[6] A.K. Dahle, Y.C. Lee, M.D. Nave, P.L. Schaffer, D.H. St John, J. Light Met. 1 (2001) 61–72.
[7] M. Liu, P.J. Uggowitzer, A.V. Nagasekhar, P. Schmutz, M. Easton, G.-L. Song, A. Atrens, Corros. Sci. 51 (2009) 602–619.
[8] M.K. Kulekci, Int. J. Adv. Manuf. Technol. 39 (2008) 851–865.
[9] N. Liu, J. Wang, L. Wang, Y. Wu, L. Wang, Corros. Sci. 51 (2009) 1328–1333.
[10] W. Liu, F. Cao, L. Chang, Z. Zhang, J. Zhang, Corros. Sci. 51 (2009) 1334–1343.
[11] J.H. Nordlien, K. Nisancioglu, S. Ono, N. Masuko, J. Electrochem. Soc. 144 (1997) 461–466.